Published in final edited form as:
Mol Cancer Res. 2014 November ; 12(11): 1644–1654. doi:10.1158/1541-7786.MCR-14-0128-T.

G protein-coupled estrogen receptor (GPER) regulates mammary tumorigenesis and metastasis

Nicole A. Marjon, **Chelin Hu**, **Helen J. Hathaway**[#], and **Eric R. Prossnitz**[##]
Department of Cell Biology & Physiology, and UNM Cancer Center, University of New Mexico Health Sciences Center, Albuquerque, NM 87131

[#] These authors contributed equally to this work.

Abstract

The role of 17β-estradiol (E2) in breast cancer development and tumor growth has traditionally been attributed exclusively to the activation of ERα. Although targeted inhibition of ERα is a successful approach for patients with ERα$^+$ breast cancer, many patients fail to respond or become resistant to anti-estrogen therapy. The discovery of the G protein-coupled estrogen receptor (GPER1) suggested an additional mechanism through which E2 could exert its effects in breast cancer. Studies have demonstrated clinical correlations between GPER expression in human breast tumor specimens and increased tumor size, distant metastasis, and recurrence, as well as established a proliferative role for GPER *in vitro*; however, direct *in vivo* evidence has been lacking. To this end, a GPER null mutation [GPER knockout (KO)] was introduced, through interbreeding, into a widely used transgenic mouse model of mammary tumorigenesis [MMTV-PyMT (PyMT)]. Early tumor development, assessed by the extent of hyperplasia and proliferation, was not different between GPER wild-type/PyMT (WT/PyMT) and those mice harboring the GPER null mutation (KO/PyMT). However, by 12-13 weeks of age, tumors from KO/PyMT mice were smaller with decreased proliferation compared to those from WT/PyMT mice. Furthermore, tumors from the KO/PyMT mice were of histologically lower grade compared to tumors from their WT counterparts, suggesting less aggressive tumors in the KO/PyMT mice. Finally, KO/PyMT mice displayed dramatically fewer lung metastases compared to WT/PyMT mice. Combined, these data provide the first *in vivo* evidence that GPER plays a critical role in breast tumor growth and distant metastasis.

Keywords

Estrogen; Receptors; Breast; Tumorigenesis; Metastasis

[#]Address Correspondence to: Eric R. Prossnitz, Department of Cell Biology & Physiology, University of New Mexico, Albuquerque, NM 87131. Tel: 505-272-5647; Fax: 505-272-1421; eprossnitz@salud.unm.edu.

Disclosures

E.R.P. holds a US patent on GPER-selective agonists and antagonists.
E.R.P. holds US patents on GPER-selective ligands and imaging agents.

Introduction

The steroid hormone 17β-estradiol (estrogen, E2) is the primary female sex hormone necessary for the development of secondary sexual characteristics in women. Specifically, E2 mediates the development of breast tissue during puberty and pregnancy by enhancing the proliferation of ductal epithelial cells. Similar to normal development, E2 also promotes breast cancer by augmenting proliferation, migration, and invasion of breast tumor cells, which has been demonstrated both *in vitro* and *in vivo* (1). By inhibiting the activity of the classical estrogen receptor ERα, many cancer-promoting effects of E2 in cultured cells and mice are reduced; therefore, the actions of E2 in breast cancer have been attributed almost exclusively to ERα (2). Clinically, drugs that block the production of estrogen or inhibit ERα, thereby inhibiting E2 signaling, increase long-term survival in patients with breast cancer (3). One of the most commonly prescribed adjuvant treatments for breast cancer is tamoxifen, a selective estrogen receptor modulator (SERM) that acts as an antagonist for ERα in the breast, inhibiting tumor growth. Treatment with tamoxifen for 5 years following surgery decreases mortality from breast cancer by approximately 30% (3), although the incidence of endometrial cancer increases by 2-4-fold (4). However, only patients with $ERα^+$ tumors are eligible for treatment, and many $ERα^+$ tumors either do not respond to tamoxifen, or become resistant during treatment or upon recurrence (5). While anti-estrogens have been highly successful, breast cancer is still the second most common cause of cancer-related death in women in the US (6). Additionally, aromatase inhibitors, which inhibit the production of E2, are more efficacious in the prevention and treatment of breast cancer compared to tamoxifen (7), indicating the inhibition of E2 signaling solely through targeting ERα may be suboptimal. Therefore, other E2 receptors may contribute to the initiation and/or progression of breast cancer.

G protein-coupled estrogen receptor (GPER, formerly GPR30) is a novel estrogen receptor with multiple functions in diverse tissues (8-12), whose role in breast carcinogenesis has yet to be directly determined (13, 14). E2 stimulation of cells expressing GPER but lacking ERα activates the MAPK and PI3K cascades, among other pathways, increasing proliferation of many breast cancer cell lines, suggesting GPER may play a role in one or more events of breast carcinogenesis (15-17) and particularly triple negative breast cancer (18, 19). A small number of retrospective studies has examined the relationship between GPER expression in breast tumor samples and clinical outcome or its correlates. A study of 361 breast cancer patients found GPER expression associated with increased primary tumor size and the prevalence of distant metastasis (20). Another investigation demonstrated an increased recurrence rate in $GPER^+$ invasive ductal breast cancers (21). More recently, a study of invasive breast cancer samples demonstrated GPER expression is an independent prognostic factor for decreased disease-free survival in patients treated exclusively with tamoxifen (22), with its cellular localization potentially playing a critical role (18). While these studies suggest a role for GPER in breast cancer, to this point no direct experimental evidence demonstrates a functional role for GPER in the initiation and/or progression of breast cancer.

In this study, we investigated the contribution of GPER to breast carcinogenesis by introducing a GPER null mutation (GPER KO) (23, 24) onto a transgenic mouse model of

mammary tumorigenesis through interbreeding. MMTV-PyMT (PyMT) transgenic mice express the polyoma middle T antigen (PyMT) primarily in mammary tissue, under control of the mammary tumor virus (MMTV) promoter, resulting in the spontaneous development of mammary tumors (25). PyMT mice on the FVB background develop hyperplastic lesions in their mammary glands by 4 weeks of age that progress through the stages of adenoma, early carcinoma and late carcinoma over the subsequent 8-10 weeks (26). Histologically, PyMT tumors at each stage of development closely resemble equivalent stage human tumors. Furthermore, changes in biomarkers during PyMT mammary tumor development are similar to human breast cancer as tumors progress from hyperplasia to carcinoma. The biomarker changes include loss of ERα, progesterone receptor and integrin β expression, as well as an increase in the expression of Neu and cyclin D1 (26). Finally, analogous to human breast cancer, early tumor growth in PyMT mice is stimulated by E2, demonstrating the PyMT model of mammary carcinogenesis to be a highly clinically relevant model of human breast cancer (27).

Using the PyMT model, we demonstrate that the presence of GPER promotes growth and metastasis of late stage mammary tumors in PyMT mice, although we observed no difference in tumor latency between GPER WT PyMT (WT/PyMT) and GPER KO PyMT (KO/PyMT) mice. Further, early development of hyperplasia was not affected by GPER expression; however, as the tumors progress, KO/PyMT mice displayed smaller tumors that exhibited a lower grade when compared to WT/PyMT and GPER heterozygous (HET/PyMT) mice. Consistent with decreased size, tumors from KO/PyMT mice displayed reduced proliferation compared to tumors from WT/PyMT mice. Perhaps most importantly, KO/PyMT mice exhibited fewer lung metastases compared to WT/PyMT mice. Taken together, these data demonstrate that silencing GPER decreases tumor size and the number of distant metastases, suggesting that pharmacological inhibition of GPER may represent a novel approach to reduce morbidity and mortality from breast cancer.

Methods

Mice

FVB/N-Tg(MMTV-PyVT)634Mul/J (MMTV-PyMT) mice were purchased from The Jackson Laboratory (Bar Harbor, ME). Mice lacking the GPER gene through targeted deletion (GPER KO) were provided by Jan Rosenbaum (Proctor & Gamble, Cincinnati, OH) and have been described previously (24). GPER KO mice were backcrossed 10 generations onto FVB/NJ mice that were purchased from Harlan Laboratories (Indianapolis, IN). GPER KO mice were intercrossed with MMTV-PyMT mice to produce MMTV-PyMT mice that were wild type (WT), heterozygous (HET), or null (knock out, KO) with respect to GPER. Animals were housed at the Animal Research Facility at the University of New Mexico Health Sciences Center and maintained under a controlled temperature of 22–23 °C with a 12-h light, 12-h dark cycle and were fed a soy-free (phytoestrogen-reduced) chow *ad libitum*. All procedures were approved by the University of New Mexico Institutional Animal Care and Use Committee and carried out in accordance with the National Institutes of Health Guide for the Care and Use of Laboratory Animals.

Tumor and lung resection

Tumors were allowed to grow until mice were 7 weeks or 12-13 weeks of age. Tumors and lungs were then resected, fixed in 4% PFA, and paraffin embedded for subsequent analysis. Hyperplastic mammary glands from 7-week-old mice were analyzed for the extent of hyperplasia and proliferation, while tumors from 12-13-week-old mice were assessed for weight (as a measurement of tumor size), proliferation rate, grade, extent of necrosis, and ERα expression. Additionally, lungs from 12-13-week-old mice were analyzed for the number of metastatic foci.

Ovariectomy

Ovariectomy was performed at 3 weeks of age. PyMT mice were anesthetized with isofluorane. A small incision was made through the skin on the dorsal midline just cranial to the hipbones. Bilateral incisions were made through the underlying muscle lateral to the spine and each ovary was removed. The muscle incisions were closed using polydioxanone synthetic absorbable sutures (PDS* Plus, Ethicon) and the skin incision was closed with 9 mm stainless steel tissue clips (ez CLIPS, Stoelting).

Tamoxifen treatment

When PyMT mice were 4-weeks-old, a 60-day release pellet containing tamoxifen (5 mg/pellet, Innovative Research of America) was subcutaneously implanted on the left dorsal side of the mouse just below the rib cage. Tumors were resected at 12 weeks of age and weighed as a measurement of tumor size.

Relative quantitation of PyMT gene expression

Mammary tumors from 13-14-week-old intact or ovariectomized PyMT mice and 10-week-old WT/PyMT and KO/PyMT were removed and homogenized in Trizol (Sigma-Aldrich) using a Polytron tissue homogenizer. RNA isolation was performed in Trizol using phenol-chloroform extraction according to the manufacturers instructions. cDNA was created via reverse transcription of 1 μg RNA with the iScript cDNA synthesis kit (BioRad) using the GeneAmp PCR system 9700 (Applied Biosystems, Inc.) according to manufacturers directions. Quantification of PyMT mRNA relative to cytokeratin 18 mRNA was performed using Fast SYBR Green (Molecular Probes) with the 7500 Fast Real-Time PCR System (Applied Biosystems, Inc). A relative standard curve for each primer pair was created from a mixture of the sample RNA extracted from the tumors with dilution values of 1.0, 0.25, 0.0625, and 0.0156. The relative concentrations were expressed as arbitrary units and plotted against the logarithm (base 10) of the dilution values. Linear regression was used to create a standard curve. The standard curves were used to determine the relative amount of PyMT and cytokeratin 18 in each sample. The relative concentration of PyMT was then normalized to the relative concentration of cytokeratin 18, which served as the endogenous control. The primer sequences were: PyMT Forward: 5′- CGG CGG AGC GAG GAA CTG AGG AGA G -3′ and Reverse: 5′- C TCT CCT CAG TTC CTC GCT CCG CCG -3′; and Cytokeratin 18 Forward: 5′- CAA GTC TGC CGA AAT CAG GGA C -3′ and Reverse: 5′- G TCC CTG ATT TCG GCA GAC TTG -3′.

Tumor histology

The largest tumors from 12-13-week-old mice were sectioned (5 μm) and stained with hematoxylin (Sigma-Aldrich) and Eosin (RICCA Chemical Company). Tumor grade was determined in a blinded manner by a veterinary pathologist (Donna Kusewitt, DVM, PhD at The University of Texas MD Anderson Cancer Center). PyMT tumor grade was determined as previously described (26) by tissue architecture, degree of cellular atypia, and invasion into the surrounding stroma. Based on these parameters, tumors were assigned grades as follows: (1) Hyperplasia: Densely packed acini filled or bridged by epithelial cells that have little to no cellular atypia with no invasion into the surrounding stroma. (2) Adenoma/ mammary intraepithelial neoplasia (MIN): Increased proliferation of epithelial cells with acini mostly filled with cells. Minimal cellular atypia and no invasion is present. (3) Early carcinoma: Florid proliferation with loss of acinar definition. Moderate cellular atypia and early stromal invasion is present. (4) Late carcinoma: Solid sheets of cells with very few or no acini present and a high mitotic index consistent with increased proliferation. Marked cellular atypia and pronounced stromal invasion are present. Sections were imaged with a Nikon DS-Fi1 camera mounted on a Nikon Eclipse E400 microscope running NIS-Elements software.

The extent of tumor necrosis was determined and categorized by the number and size of necrotic areas as follows: 1 = few small areas; 2 = few larger areas or moderate number of smaller areas; 3 = extensive areas.

Immunostaining analysis

For immunostaining, 5 μm sections were deparaffinized, rehydrated, permeabilized in PBS containing 0.01% Triton X-100, and blocked in 3% normal goat serum (NGS) diluted in PBS plus 0.1% Tween-20 (PBS-T).

To evaluate cellular proliferation rate, microwave antigen retrieval was performed in 0.1 M sodium citrate (pH 6). Sections were incubated overnight in a 1:100 dilution of the anti-phospho-histone H3 (P-histone H3, phospho Ser10, EMD Millipore) followed by detection with an anti-rabbit IgG antibody conjugated to Alexa 488 (Molecular Probes). Coverslips were mounted with Vectashield mounting medium with 4′,6-diamidino-2-phenylindole (DAPI, Vector Laboratories). One random field from 3 sections was imaged with a Zeiss 200M Axiovert microscope using MetaMorph® software. In a blinded manner, the number of P-histone H3-positive cells was determined and normalized to the total number of cells per field. Apoptosis was evaluated in the same manner, except the primary antibody was directed against cleaved caspase-3 (Asp 175, Cell Signaling).

To detect ERα, microwave antigen retrieval was performed in TET buffer (10mM Tris, 1mM EDTA, 0.05% Tween-20; pH 9) and endogenous peroxide activity was quenched in 3% H_2O_2 before permeabilization. Sections were incubated overnight in a 1:100 dilution of anti-ERα antibody (MC-20, Santa Cruz Biotechnology). The sections were washed in PBS-T and incubated with anti-rabbit IgG antibody conjugated to horseradish peroxidase (HRP, Molecular Probes). 3,3′-Diaminobenzidine (DAB, Sigma-Aldrich) was used as the substrate to detect the presence of the HRP-conjugated antibody. Coverslips were mounted with

Permount mounting medium (Fisher Scientific). Three random fields per section were imaged with a Nikon DS-Fi1 camera mounted on a Nikon Eclipse E400 microscope running NIS-Elements software. The number of ERα-positive cells was determined and normalized to the total number of cells per field.

Lung metastasis

Three 5 μm sections separated by 100 μm were prepared from the lungs of 12-13-week-old animals. Sections were deparaffinized, rehydrated, and stained with H&E. Metastatic tumor foci present in the lung parenchyma are defined as a tightly clustered group of 10 or more hematoxylin-positive cells that excludes eosin-stained stroma. Total metastatic foci were counted in the three lung sections to determine the extent of metastasis. The counting was blinded to the investigator with respect to the genotype.

Whole Mount

Number 4 abdominal mammary glands from 7-week-old PyMT mice were fixed in 4% PFA on stretched skin overnight at room temperature. The glands were removed from the skin, incubated overnight in 100% acetone to remove the fat, washed in deionized water, and stained with carmine (Sigma-Aldrich) overnight as described (http://mammary.nih.gov). After staining, the glands were washed in deionized water and dehydrated in ethanol before storing in methyl salicylate (Sigma Aldrich). Glands were imaged with MoticCam 2300 running Motic software on an Olympus SZH dissection microscope.

Statistical Analysis

Differences in tumor size in ovariectomized and tamoxifen treated mice, hyperplasia in 7-week glands, P-histone H3 positive cells, relative concentration of PyMT RNA, ERα expression, and extent of lung metastasis were evaluated using two-tailed student's t-test with a p-value threshold for significance of 0.05. Differences in tumor size of WT/PyMT, HET/PyMT and KO/PyMT mice were assessed using one-way ANOVA with Bonferroni correction for multiple comparisons as a post-hoc test. Tumor grade and extent of necrosis were analyzed using a two-tailed Fisher's exact test with a p-value threshold for significance of 0.05. Correlation between ERα and tumor grade was assessed using Pearson's correlation analysis with a p-value threshold for significance of 0.05.

Results

Ovariectomy and tamoxifen treatment reduce mammary tumor size

Although GPER expression has been correlated with human breast tumor growth and metastasis, *in vivo* studies determining the effects of GPER on breast cancer initiation, growth, and progression have not been reported. To study the role of GPER in breast cancer, we used the MMTV-PyMT (PyMT) model of mammary carcinogenesis, which has been described to be an E2-responsive tumor model (27). To verify the E2-responsiveness of tumor growth, PyMT mice were ovariectomized to remove the majority of circulating estrogen. The size of tumors from ovariectomized mice was compared to tumors from non-ovariectomized mice at 12 weeks of age. Mammary glands were palpated two times per week to detect the presence of tumors. Both cohorts of mice developed tumors between 7

and 8 weeks of age, suggesting there was no apparent effect of ovariectomy on tumor latency. However, by 12 weeks of age, the tumors in the ovary-intact mice were 5-fold larger than those in the ovariectomized mice (Figure 1A), indicating tumor growth in PyMT mice is highly dependent on the presence of ovaries, suggesting E2-responsiveness. While steroid hormones such as glucocorticoids, progestins, and androgens stimulate the MMTV promoter and increase the expression of PyMT in this transgenic model (28), E2 treatment has repeatedly been shown to have no effect on the expression of PyMT (29, 30). To assess whether E2 withdrawal, either directly or indirectly through the modulation of other hormones, might affect the expression of PyMT through the MMTV promoter and thereby directly modulate tumor size, we evaluated PyMT expression in the tumors from the ovary-intact and ovariectomized mice. PyMT expression in mammary tumors was not different between intact and ovariectomized mice (1.00 ± 0.24 vs. 1.33 ± 0.39, $n=6$, $p = 0.49$), verifying the effects of ovariectomy on tumor size likely result from decreased E2 signaling and not decreased PyMT expression To further examine the role of E2 signaling, we next examined the effect of ERα-dependent activity on tumor size employing subcutaneously implanted tamoxifen pellets in 4-week-old PyMT mice to block E2-mediated effects through ERα. When mice were 12 weeks of age, tumors were resected and weighed. Tumors from mice treated with tamoxifen were about 3.5-fold smaller than tumors from sham-treated mice, demonstrating estrogen receptor specificity (Figure 1B). Additionally, as ovariectomy was more effective than tamoxifen at decreasing tumor size, ERα may not be the only estrogen receptor regulating tumor growth. We also concluded that, because of its E2 responsiveness, this model would be appropriate for examining the role of GPER in mammary tumorigenesis.

GPER deficiency does not affect tumor initiation or early tumor proliferation

GPER WT, HET, and KO mice on a PyMT background (WT/PyMT, HET/PyMT, KO/PyMT, respectively) were generated. Tumors in both WT/PyMT and KO/PyMT mice were palpable between 7 and 8 weeks of age, suggesting no difference in tumor latency. To assess differences in early tumor development, whole mounts of the number 4 abdominal mammary glands from 7-week-old WT/PyMT and KO/PyMT mice were stained with carmine to determine the extent of hyperplasia as follows. In Image J, a grid was overlaid on the whole mount images and each box was evaluated for the presence of hyperplasia and epithelium (Figure 2A). The total area of hyperplasia relative to the total area of epithelium was 0.73 ± 0.05 for WT/PyMT and 0.64 ± 0.05 for KO/PyMT, demonstrating no statistical difference ($p > 0.05$) (Figure 2B). To determine whether the lesions in WT/PyMT mice had extended farther into the mammary gland than in KO/PyMT mice, indicating more advanced disease, hyperplasia distal to the midline of the lymph node relative to total epithelium distal to the midline of the lymph node was also evaluated. No difference was evident in the extent of hyperplasia distal to the lymph node between WT/PyMT ($0.41 \pm .08$) and KO/PyMT ($0.34 \pm .07$) mice ($p > 0.05$) (Figure 2C). Proliferation in early tumors was then examined by staining number 2/3 mammary glands from 7-week-old mice with an anti-phospho-histone H3 (P-histone H3) antibody, a marker of the M phase of the cell cycle. No difference in the number of proliferating cells between tumors from WT/PyMT (4/500 cells) and KO/PyMT (3/500 cells) mice ($p > 0.05$) was evident (Figure 2D). Collectively, these data indicate that

the absence of GPER does not significantly reduce the development or growth of early mammary tumors.

Late-stage mammary tumor growth is reduced in the absence of GPER

Although early tumor development was not altered in the absence of GPER, tumors from older mice were evaluated to determine if GPER expression affects the progression of more advanced tumors. When mice were 12-13-weeks-old, tumors were removed and weighed as a measure of tumor size. Although there was no difference between WT/PyMT and HET/PyMT (0.26 ± 0.02 vs. 0.26 ± 0.01, $p = 0.79$) tumor size, tumors from KO/PyMT mice were 28% smaller than those from WT/PyMT mice ($p < 0.05$) (Figure 3A). To verify the difference in tumor mass was not indirectly caused by decreased PyMT expression in KO/PyMT mice, real time PCR was used to determine the level of PyMT mRNA expression relative to cytokeratin 18, a marker of epithelial cells, in tumors from WT/PyMT and KO/PyMT mice. No difference in the relative expression of PyMT RNA between WT/PyMT and KO/PyMT mice was detected ($p > 0.05$), indicating differences in tumor mass were not an indirect result of decreased PyMT expression (Figure 3B).

Because tumors in KO/PyMT mice were smaller than in WT/PyMT tumors, proliferation and apoptosis of the tumor cells were analyzed to determine the relative contribution of each factor to overall tumor size. To evaluate the proliferation rate, the number of P-histone H3-positive cells was determined and normalized to the total number of cells. Tumors from KO/PyMT mice exhibited 44% fewer P-histone H3-positive cells than tumors from WT/PyMT mice ($p < 0.05$) (Figure 3C and D). Apoptosis was determined using an antibody directed against cleaved caspase-3 and similarly analyzed by microscopy. Although a positive control exhibited cleaved caspase-3 expressing cells, the tumors displayed no cleaved caspase-3-positive staining regardless of genotype (not shown). Therefore, we conclude that GPER-expressing tumors are larger, in part, due to increased tumor cell proliferation.

GPER expression is associated with predictors of poor prognosis

To determine the contribution of GPER expression to tumor aggressiveness, sections of the largest tumor from WT/PyMT and KO/PyMT mice were stained with H&E, analyzed to determine grade, and classified as either low-grade (hyperplasia and adenoma) or high-grade (early and late carcinoma) (Figure 4A). The majority of tumors from WT/PyMT mice lost acinar definition appearing as solid sheets of cells, and had invaded through the basement membrane into the surrounding stroma, indicative of carcinoma. In contrast, tumors from KO/PyMT mice more often appeared to maintain acinar structure, although the acini were filled with cells; in addition, fewer tumors invaded through the basal lamina in the KO/PyMT mice. These histological parameters revealed that 90% of tumors from WT/PyMT mice were carcinomas versus 50% of tumors from KO/PyMT mice, demonstrating a strong trend for KO/PyMT tumors to exhibit a lower tumor grade than WT/PyMT tumors ($p = .056$) (Figure 4B).

During tumor resection, it appeared that tumors from KO/PyMT mice contained a smaller necrotic center than WT/PyMT mice. Because necrosis is an independent predictor for poor prognosis, a smaller necrotic center suggests less aggressive tumors (31). Necrosis was

analyzed by evaluating the number and size of necrotic areas categorized using a scale from 0-3 with 0 signifying a lack of necrosis and 3 representing large and/or many areas of necrosis. The majority of tumors (78%) from WT/PyMT mice were scored 2 or greater compared with 21% of tumors from KO/PyMT mice receiving a score of 2 and no tumors from KO/PyMT mice receiving the highest score of 3 (Figure 4C). Thus, tumors lacking GPER exhibit fewer and smaller areas of necrosis compared to tumors that express GPER ($p < 0.05$). These data suggest that loss of GPER in KO/PyMT mice leads to less aggressive tumors than mice with normal levels of GPER.

ERα expression is unaffected by GPER deficiency

As ERα drives proliferation in approximately 70% of human breast tumors and tamoxifen successfully inhibited PyMT tumor growth, we considered that eliminating GPER could affect the expression of ERα in the tumors of PyMT mice, thus indirectly affecting tumorigenesis (32). To examine ERα expression, sections of hyperplastic mammary glands from 7-week-old and 12-13-week-old mice were stained and analyzed for the number of $ERα^+$ cells as well as staining intensity. Hyperplastic glands from 7-week-old mice displayed faint ERα staining in the hyperplastic/adenomatous regions, and intense staining in the adjacent normal tissue, suggesting that as tumors form, ERα expression begins to decrease (Figure 5A), in agreement with published observations (26). The number of $ERα^+$ cells quantitated in three random fields was not different between mammary glands from 7-week-old WT/PyMT and KO/PyMT mice (Figure 5B). Tumors from 12-13-week-old mice displayed faint ERα immunostaining that was less intense than that of 7-week hyperplastic tissue (Figure 5A). Consistent with immunostaining in 7-week mammary glands, the number of ERα-expressing cells in tumors from 12-13-week-old mice was similar in WT/PyMT and KO/PyMT mice (Figure 5C). Thus, manipulating the expression of GPER does not affect the expression of ERα. Because patients with $ERα^+$ tumors have a better prognosis than those with $ERα^-$ tumors, the number of ERα-expressing cells in tumors from 12-13-week-old WT/PyMT and KO/PyMT tumors was analyzed with respect to tumor grade. Consistent with patient data, higher ERα expression correlated with a lower tumor grade ($p = 0.05$) (Figure 5D).

GPER deficiency yields fewer metastases to the lung

While tumor size, grade, proliferation rate, and estrogen receptor status are predictive of aggressiveness in breast tumors, the most reliable predictor of survival in patients is the presence of distant metastases (33, 34). The most common metastatic sites for human breast cancer are the lungs, liver, and bone (35). PyMT tumors predominantly metastasize to the lung, thus representing an appropriate model of human breast cancer for the evaluation of metastasis (1). To assess the extent of metastasis, lungs of 12-13-week-old KO/PyMT and WT/PyMT mice were stained with H&E and the number of tumor foci, designated as a group of 10 or more densely packed cells, was determined in 3 lung sections separated by 100 μm (Figure 6A). Lungs from WT/PyMT mice contained 9.0 ± 1.9 metastatic foci while lungs from KO/PyMT mice contained 3.8 ± 0.69 metastatic foci, representing a 2.4-fold reduction in metastases in KO/PyMT mice ($p < 0.05$) (Figure 6B). While the majority of mice had metastasis at this age, 83% of KO/PyMT mice had fewer than 5 metastases in the analyzed lung tissue compared to 33% of WT/PyMT mice (Figure 6C). Together, these data

demonstrate that PyMT mice lacking GPER have a substantially decreased incidence of metastasis.

Discussion

Several reports have demonstrated that multiple cancer cell lines proliferate in response to the GPER-selective agonist G-1 (36-38) and that E2-dependent proliferation can be reduced upon silencing GPER expression or inhibiting GPER activity (16, 39-41). While these data suggest GPER may promote breast tumor growth, its importance in breast cancer initiation, growth and progression has remained unexplored. This report is therefore the first to describe a role for GPER in both tumor progression and metastasis using an *in vivo* model of breast carcinogenesis.

In this study, WT/PyMT and KO/PyMT mice were compared to determine the effects of GPER on *in vivo* mammary tumor growth and metastasis. Assessment of tumor initiation and early proliferation revealed no GPER-dependent effect. However, in more advanced disease, tumors from KO/PyMT mice were smaller than tumors from WT/PyMT mice, due in part to decreased tumor cell proliferation, suggesting a role for GPER in the proliferation and growth of mammary tumors. Although the mechanism of proliferation was not elucidated *in vivo*, many *in vitro* models give insight into the mechanisms of GPER-mediated proliferation. GPER has been demonstrated to regulate cellular proliferation in many cancer cell types including, breast, endometrial, and ovarian cancer cells through transactivation of the EGFR, resulting in increased ERK1/2 activation and transcription of genes including cyclins D1, E and A, c-fos and egr-1 (37, 38, 42). Secondly, GPER is involved in the E2-dependent activation of fibroblasts in the tumor microenvironment (43-47). Activated fibroblasts act to enhance the growth and metastasis of tumors *in vivo*. Therefore, GPER expression in both the tumor and microenvironment may contribute to the increased tumor size in WT/PyMT mice.

Although it is unclear why the loss of GPER did not affect early tumor proliferation, we suggest the delay in effects of GPER deficiency may be due to the classical E2 receptor ERα. ERα dramatically increases the proliferation rate and growth of breast tumors, although its role in the PyMT model has been debated (48). We demonstrated that the growth of PyMT tumors is sensitive to both early estrogen deprivation and tamoxifen administration, strongly suggesting a role for ERα in tumor initiation and proliferation. However, the expression of ERα was largely lost as tumors progressed, with early hyperplastic lesions demonstrating higher ERα expression compared to later stage carcinomas, suggesting ERα expression and function are integral to the early proliferation of neoplastic cells in this model, with diminishing effects as its expression decreases. Therefore, we propose that ERα plays a dominant role in early mammary tumor development through its robust proliferative effects, mitigating the effects of GPER expression or lack thereof at early stages. Therefore, the growth-promoting effects of GPER may become more important in later tumor development and progression as those of ERα decline.

While tumor size is predictive of more aggressive disease, metastasis is the most important predictor of morbidity and mortality in women with breast cancer (49). We demonstrated that KO/PyMT mice have fewer metastases compared with WT/PyMT mice, indicating that GPER plays a role in mammary tumor cell metastasis consistent with previous *in vitro* (16, 44, 50, 51) and clinical data (20). Several possible mechanisms have been observed for GPER-dependent tumor cell migration and invasion. *In vitro* studies have demonstrated GPER-dependent invasion through a recombinant basement membrane due to increased MMP-9 expression and activation (52), one of the first steps of metastasis. Furthermore, *in vitro* migration is enhanced through GPER activation in tumor cells as well as cells in the microenvironment, specifically fibroblasts, through induction of CTGF expression. Increased CTGF expression is critical for stimulating cell migration (45). While these mechanisms have been described for GPER mediating tumor cell “escape” from their local environment, the role of GPER at the site of distant metastasis has not been examined. Tumor cell metastasis to distant sites cannot be successful unless the invasive tumor cells can survive and proliferate in the new environment. Therefore, it is important to determine if GPER augments metastasis through enhancing the ability of cells to escape the tumor microenvironment, supporting the ability of tumor cells to survive and grow in a novel environment, or both. Understanding the mechanisms of GPER-mediated metastasis will enhance our ability to effectively target GPER to inhibit metastasis.

While these *in vitro* data have given insight into the possible role(s) of GPER in breast cancer aggressiveness, it is important to recognize that clinical studies have also demonstrated a correlation between GPER expression and tumor size, metastasis, and recurrence. In one retrospective analysis by Filardo and colleagues, high GPER expression in breast tumors correlated with larger tumor size and increased distant metastasis, consistent with results of this study. Furthermore, it has been proposed that GPER plays a role in tamoxifen resistance and recurrence following tamoxifen therapy. While tamoxifen is a selective estrogen receptor modulator (SERM) that inhibits ERα in the breast, it ubiquitously activates GPER, possibly contributing to tamoxifen resistance and the development of tamoxifen-associated uterine cancer (53). In a retrospective study, Ignatov and colleagues demonstrated that in patients treated with tamoxifen as a monotherapy, high GPER expression correlated with subsequent tamoxifen resistance and decreased relapse-free survival (22). Therefore, administering a GPER-selective antagonist following or in combination with tamoxifen could represent an approach to inhibit resistance and improve the efficacy of tamoxifen and other SERMs (40, 53). Furthermore, tamoxifen is only effective in patients with ERα-positive tumors, leaving ~30% of breast cancer patients with fewer treatment options (32). However, 60% of patients with ERα-negative tumors express GPER (20, 22) that may be enhancing tumor growth and metastasis, providing a novel therapeutic target in these patients. Given the possible roles of GPER in tamoxifen-resistant and ERα-negative tumors, GPER is an appealing target to reduce tumor growth and metastasis, especially in premenopausal women who are not candidates for aromatase inhibitor therapy.

In conclusion, this is the first *in vivo* study to demonstrate a role for GPER in the progression of breast cancer, identifying a novel target for hormone therapy in breast cancer.

As GPER is expressed in 60% of ERα-negative tumors, targeting GPER could increase patient survival in women with the more aggressive ERα-negative tumors. GPER expression is also associated with increased recurrence after adjuvant treatment with tamoxifen as a monotherapy (20, 22), and, therefore, may be an effective therapeutic target in combination with tamoxifen or other SERMs. Finally, as GPER-selective small molecule inhibitors (G15 and G36) (54, 55) have been developed and safely administered to mice, GPER represents an even more attractive clinical target. Based on an extensive body of evidence, GPER has been demonstrated *in vitro*, in clinical studies, and now for the first time in an *in vivo* animal model to be an important player in the growth and metastasis of breast cancer, thus representing an important new therapeutic target for breast cancer treatment.

Acknowledgments

Financial Support: This study was supported by NIH grants CA116662 and CA163890 (ERP), the New Mexico Cowboys for Cancer Research Foundation (ERP); and a predoctoral fellowship from the Department of Defense Breast Cancer Research Program BC093957 (NAM).

References

1. Fantozzi A, Christofori G. Mouse models of breast cancer metastasis. Breast Cancer Res. 2006; 8:212. [PubMed: 16887003]
2. Higa GM, Fell RG. Sex Hormone Receptor Repertoire in Breast Cancer. Int J Breast Cancer. 2013; 2013:284036. [PubMed: 24324894]
3. Early Breast Cancer Trialists' Collaborative Group: Effects of chemotherapy and hormonal therapy for early breast cancer on recurrence and 15-year survival: an overview of the randomised trials. Lancet. 2005; 365:1687–717. [PubMed: 15894097]
4. Polin SA, Ascher SM. The effect of tamoxifen on the genital tract. Cancer Imaging. 2008; 8:135–45. [PubMed: 18603495]
5. Ali S, Coombes RC. Endocrine-responsive breast cancer and strategies for combating resistance. Nat Rev Cancer. 2002; 2:101–12. [PubMed: 12635173]
6. Siegel R, Naishadham D, Jemal A. Cancer statistics, 2012. CA Cancer J Clin. 2012; 62:10–29. [PubMed: 22237781]
7. Dowsett M, Cuzick J, Ingle J, Coates A, Forbes J, Bliss J, et al. Meta-analysis of breast cancer outcomes in adjuvant trials of aromatase inhibitors versus tamoxifen. J Clin Oncol. 2010; 28:509–18. [PubMed: 19949017]
8. Sharma G, Prossnitz ER. Mechanisms of estradiol-induced insulin secretion by the G protein-coupled estrogen receptor GPR30/GPER in pancreatic beta-cells. Endocrinology. 2011; 152:3030–9. [PubMed: 21673097]
9. Prossnitz ER, Barton M. Estrogen biology: New Iinsights into GPER function and clinical opportunities. Mol Cell Endocrinol. 2014 in press.
10. Brunsing RL, Owens KS, Prossnitz ER. The G protein-coupled estrogen receptor (GPER) agonist G-1 expands the regulatory T-cell population under TH17-polarizing conditions. J Immunother. 2013; 36:190–6. [PubMed: 23502766]
11. Filardo EJ, Thomas P. Minireview: G protein-coupled estrogen receptor-1, GPER-1: its mechanism of action and role in female reproductive cancer, renal and vascular physiology. Endocrinology. 2012; 153:2953–62. [PubMed: 22495674]
12. Prossnitz ER. G protein-coupled estrogen receptor: a new therapeutic target in stroke and traumatic brain/spinal cord injury? Crit Care Med. 2012; 40:3323–5. [PubMed: 23164781]
13. Prossnitz ER, Barton M. The G-protein-coupled estrogen receptor GPER in health and disease. Nat Rev Endocrinol. 2011; 7:715–26. [PubMed: 21844907]

14. Prossnitz ER, Arterburn JB, Smith HO, Oprea TI, Sklar LA, Hathaway HJ. Estrogen signaling through the transmembrane G protein-coupled receptor GPR30. Annu Rev Physiol. 2008; 70:165–90. [PubMed: 18271749]
15. Filardo EJ, Quinn JA, Bland KI, Frackelton AR Jr. Estrogen-induced activation of Erk-1 and Erk-2 requires the G protein-coupled receptor homolog, GPR30, and occurs via trans-activation of the epidermal growth factor receptor through release of HB-EGF. Mol Endocrinol. 2000; 14:1649–60. [PubMed: 11043579]
16. Pandey DP, Lappano R, Albanito L, Madeo A, Maggiolini M, Picard D. Estrogenic GPR30 signalling induces proliferation and migration of breast cancer cells through CTGF. EMBO J. 2009; 28:523–32. [PubMed: 19153601]
17. Revankar CM, Cimino DF, Sklar LA, Arterburn JB, Prossnitz ER. A transmembrane intracellular estrogen receptor mediates rapid cell signaling. Science. 2005; 307:1625–30. [PubMed: 15705806]
18. Samartzis EP, Noske A, Meisel A, Varga Z, Fink D, Imesch P. The G Protein-Coupled Estrogen Receptor (GPER) Is Expressed in Two Different Subcellular Localizations Reflecting Distinct Tumor Properties in Breast Cancer. PLoS One. 2014; 9:e83296. [PubMed: 24421881]
19. Girgert R, Emons G, Grundker C. Inactivation of GPR30 reduces growth of triple-negative breast cancer cells: possible application in targeted therapy. Breast Cancer Res Treat. 2012; 134:199–205. [PubMed: 22290080]
20. Filardo EJ, Graeber CT, Quinn JA, Resnick MB, Giri D, DeLellis RA, et al. Distribution of GPR30, a seven membrane-spanning estrogen receptor, in primary breast cancer and its association with clinicopathologic determinants of tumor progression. Clin Cancer Res. 2006; 12:6359–66. [PubMed: 17085646]
21. Liu Q, Li JG, Zheng XY, Jin F, Dong HT. Expression of CD133, PAX2, ESA, and GPR30 in invasive ductal breast carcinomas. Chin Med J (Engl). 2009; 122:2763–9. [PubMed: 19951611]
22. Ignatov A, Ignatov T, Weissenborn C, Eggemann H, Bischoff J, Semczuk A, et al. G-protein-coupled estrogen receptor GPR30 and tamoxifen resistance in breast cancer. Breast Cancer Res Treat. 2011; 128:457–66. [PubMed: 21607586]
23. Sharma G, Hu C, Brigman JL, Zhu G, Hathaway HJ, Prossnitz ER. GPER deficiency in male mice results in insulin resistance, dyslipidemia, and a proinflammatory state. Endocrinology. 2013; 154:4136–45. [PubMed: 23970785]
24. Wang C, Dehghani B, Magrisso IJ, Rick EA, Bonhomme E, Cody DB, et al. GPR30 contributes to estrogen-induced thymic atrophy. Mol Endocrinol. 2008; 22:636–48. [PubMed: 18063692]
25. Fluck MM, Schaffhausen BS. Lessons in signaling and tumorigenesis from polyomavirus middle T antigen. Microbiol Mol Biol Rev. 2009; 73:542–63. Table of Contents. [PubMed: 19721090]
26. Lin EY, Jones JG, Li P, Zhu L, Whitney KD, Muller WJ, et al. Progression to malignancy in the polyoma middle T oncoprotein mouse breast cancer model provides a reliable model for human diseases. Am J Pathol. 2003; 163:2113–26. [PubMed: 14578209]
27. Dabrosin C, Palmer K, Muller WJ, Gauldie J. Estradiol promotes growth and angiogenesis in polyoma middle T transgenic mouse mammary tumor explants. Breast Cancer Res Treat. 2003; 78:1–6. [PubMed: 12611451]
28. Ham J, Thomson A, Needham M, Webb P, Parker M. Characterization of response elements for androgens, glucocorticoids and progestins in mouse mammary tumour virus. Nucleic Acids Res. 1988; 16:5263–76. [PubMed: 2838812]
29. Liu B, Ordonez-Ercan D, Fan Z, Huang X, Edgerton SM, Yang X, et al. Estrogenic promotion of ErbB2 tyrosine kinase activity in mammary tumor cells requires activation of ErbB3 signaling. Mol Cancer Res. 2009; 7:1882–92. [PubMed: 19861407]
30. Otten AD, Sanders MM, McKnight GS. The MMTV LTR promoter is induced by progesterone and dihydrotestosterone but not by estrogen. Mol Endocrinol. 1988; 2:143–7. [PubMed: 2840570]
31. Leek RD, Landers RJ, Harris AL, Lewis CE. Necrosis correlates with high vascular density and focal macrophage infiltration in invasive carcinoma of the breast. Br J Cancer. 1999; 79:991–5. [PubMed: 10070902]
32. Brisken C, O'Malley B. Hormone action in the mammary gland. Cold Spring Harb Perspect Biol. 2010; 2:a003178. [PubMed: 20739412]

33. Cianfrocca M, Goldstein LJ. Prognostic and predictive factors in early-stage breast cancer. Oncologist. 2004; 9:606–16. [PubMed: 15561805]
34. Li CI, Uribe DJ, Daling JR. Clinical characteristics of different histologic types of breast cancer. Br J Cancer. 2005; 93:1046–52. [PubMed: 16175185]
35. Lorusso G, Ruegg C. New insights into the mechanisms of organ-specific breast cancer metastasis. Semin Cancer Biol. 2012; 22:226–33. [PubMed: 22504658]
36. Bologa CG, Revankar CM, Young SM, Edwards BS, Arterburn JB, Kiselyov AS, et al. Virtual and biomolecular screening converge on a selective agonist for GPR30. Nat Chem Biol. 2006; 2:207–12. [PubMed: 16520733]
37. Albanito L, Madeo A, Lappano R, Vivacqua A, Rago V, Carpino A, et al. G protein-coupled receptor 30 (GPR30) mediates gene expression changes and growth response to 17beta-estradiol and selective GPR30 ligand G-1 in ovarian cancer cells. Cancer Res. 2007; 67:1859–66. [PubMed: 17308128]
38. Vivacqua A, Romeo E, De Marco P, De Francesco EM, Abonante S, Maggiolini M. GPER mediates the Egr-1 expression induced by 17beta-estradiol and 4-hydroxitamoxifen in breast and endometrial cancer cells. Breast Cancer Res Treat. 2012; 133:1025–35. [PubMed: 22147081]
39. Liu H, Yan Y, Wen H, Jiang X, Cao X, Zhang G, et al. A novel estrogen receptor GPER mediates proliferation induced by 17beta-estradiol and selective GPER agonist G-1 in estrogen receptor alpha (ERalpha)-negative ovarian cancer cells. Cell Biol Int. 2014
40. Mo Z, Liu M, Yang F, Luo H, Li Z, Tu G, et al. GPR30 as an initiator of tamoxifen resistance in hormone-dependent breast cancer. Breast Cancer Res. 2013; 15:R114. [PubMed: 24289103]
41. Bai LY, Weng JR, Hu JL, Wang D, Sargeant AM, Chiu CF. G15, a GPR30 antagonist, induces apoptosis and autophagy in human oral squamous carcinoma cells. Chem Biol Interact. 2013; 206:375–84. [PubMed: 24161432]
42. Prossnitz ER, Maggiolini M. Mechanisms of estrogen signaling and gene expression via GPR30. Mol Cell Endocrinol. 2009; 308:32–8. [PubMed: 19464786]
43. Pupo M, Vivacqua A, Perrotta I, Pisano A, Aquila S, Abonante S, et al. The nuclear localization signal is required for nuclear GPER translocation and function in breast Cancer-Associated Fibroblasts (CAFs). Mol Cell Endocrinol. 2013; 376:23–32. [PubMed: 23748028]
44. Madeo A, Maggiolini M. Nuclear alternate estrogen receptor GPR30 mediates 17beta-estradiol-induced gene expression and migration in breast cancer-associated fibroblasts. Cancer Res. 2010; 70:6036–46. [PubMed: 20551055]
45. Pandey DP, Lappano R, Albanito L, Madeo A, Maggiolini M, Picard D. Estrogenic GPR30 signalling induces proliferation and migration of breast cancer cells through CTGF. EMBO Journal. 2009; 28:523–32. [PubMed: 19153601]
46. Luo H, Yang G, Yu T, Luo S, Wu C, Sun Y, et al. GPER-mediated proliferation and estradiol production in breast cancer associated fibroblasts. Endocr Relat Cancer. 2014
47. Pupo M, Pisano A, Abonante S, Maggiolini M, Musti AM. GPER activates Notch signaling in breast cancer cells and cancer-associated fibroblasts (CAFs). Int J Biochem Cell Biol. 2014; 46:56–67. [PubMed: 24275097]
48. Ali S, Coombes RC. Estrogen receptor alpha in human breast cancer: occurrence and significance. J Mammary Gland Biol Neoplasia. 2000; 5:271–81. [PubMed: 14973389]
49. Liu D, Chen Y, Deng M, Xie G, Wang J, Zhang L, et al. Lymph node ratio and breast cancer prognosis: a meta-analysis. Breast Cancer. 2014; 21:1–9. [PubMed: 24101545]
50. Yan Y, Liu H, Wen H, Jiang X, Cao X, Zhang G, et al. The novel estrogen receptor GPER regulates the migration and invasion of ovarian cancer cells. Mol Cell Biochem. 2013; 378:1–7. [PubMed: 23580092]
51. Ohshiro K, Schwartz AM, Levine PH, Kumar R. Alternate estrogen receptors promote invasion of inflammatory breast cancer cells via non-genomic signaling. PLoS One. 2012; 7:e30725. [PubMed: 22295107]
52. Quinn JA, Graeber CT, Frackelton AR Jr. Kim M, Schwarzbauer JE, Filardo EJ. Coordinate regulation of estrogen-mediated fibronectin matrix assembly and epidermal growth factor receptor transactivation by the G protein-coupled receptor, GPR30. Mol Endocrinol. 2009; 23:1052–64. [PubMed: 19342448]

53. Petrie WK, Dennis MK, Hu C, Dai D, Arterburn JB, Smith HO, et al. G protein-coupled estrogen receptor-selective ligands modulate endometrial tumor growth. Obstet Gynecol Int. 2013; 2013:472720. [PubMed: 24379833]

54. Dennis MK, Field AS, Burai R, Ramesh C, Petrie WK, Bologa CG, et al. Identification of a GPER/GPR30 antagonist with improved estrogen receptor counterselectivity. J Steroid Biochem Mol Biol. 2011; 127:358–66. [PubMed: 21782022]

55. Dennis MK, Burai R, Ramesh C, Petrie WK, Alcon SN, Nayak TK, et al. In vivo effects of a GPR30 antagonist. Nat Chem Biol. 2009; 5:421–7. [PubMed: 19430488]

Implications

This is the first description of a role for the novel G protein-coupled estrogen receptor GPER in breast tumorigenesis and metastasis, demonstrating that it represents a new target in breast cancer diagnosis, prognosis and therapy.

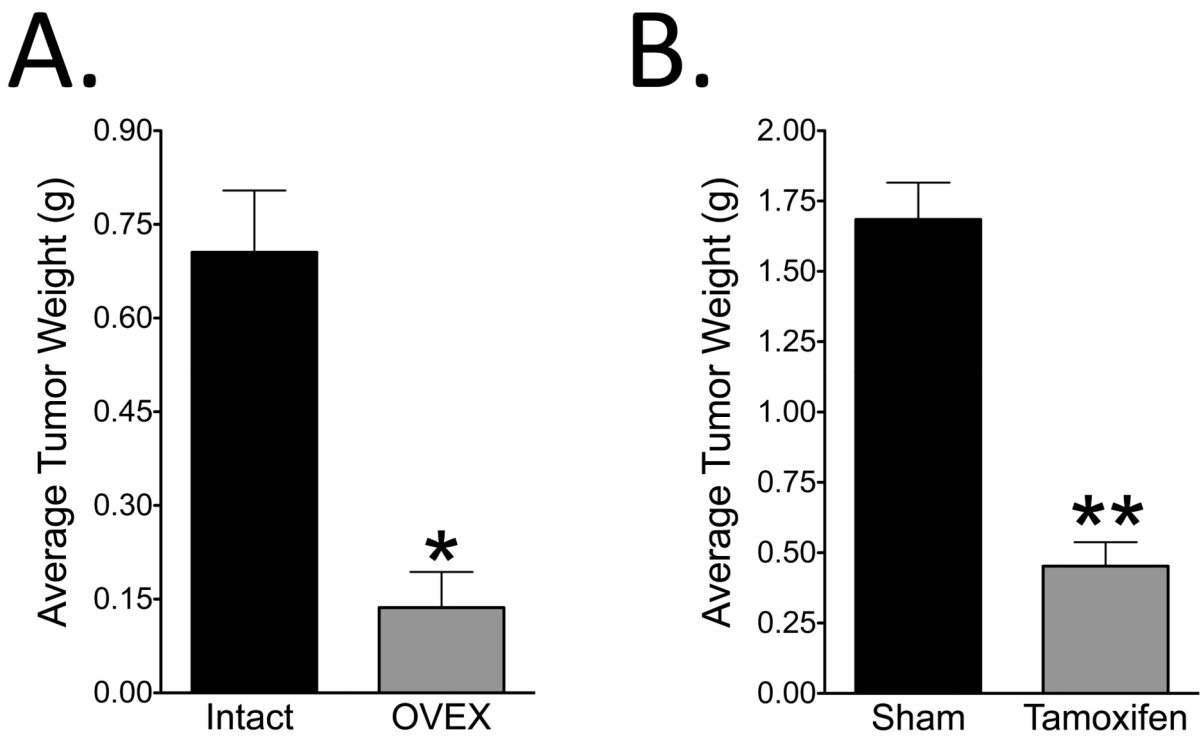

Figure 1. Estrogen enhances mammary tumorigenesis in the PyMT model

A) PyMT mice were ovariectomized at 3 weeks of age to remove the majority of circulating E2. Tumors were resected from ovariectomized (n = 5) and intact (n = 3) mice and weighed as a measure of tumor size when mice were 12 weeks old. B) 60-day release tamoxifen pellets were subcutaneously implanted into 4-week-old PyMT mice. Tumors from tamoxifen treated mice (n = 3) and sham treated mice (n = 3) were resected and weighed as a measure of tumor size when mice were 12 weeks old. Two-tailed Student's t-test with a p-value threshold of 0.05 was used for statistical analysis.

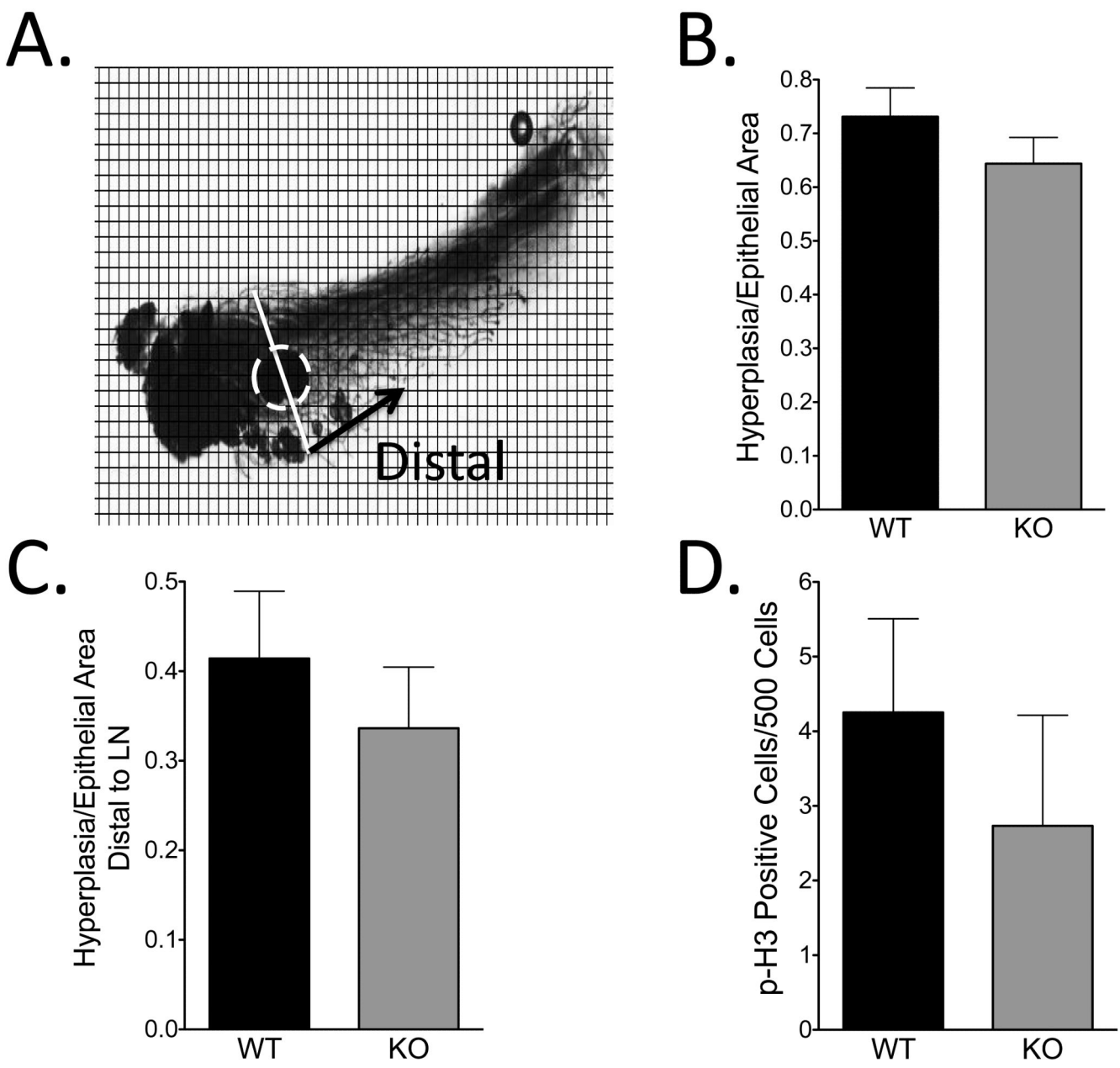

Figure 2. Absence of GPER does not affect early tumor development

A) Whole mounts of number 4 abdominal mammary glands from 7-week-old WT/PyMT (n = 9) and KO/PyMT (n = 6) mice were stained with carmine to visualize hyperplasia. Using Image J software, a grid was overlaid on the image, and each box was analyzed for the presence of hyperplasia and normal epithelium. Hyperplasia was analyzed in the total gland and distal to the lymph node (dashed circle). B) Quantification of total gland hyperplasia. The number of boxes containing hyperplasia was normalized to the number of boxes containing total epithelium, which is defined as hyperplastic and normal epithelium. C) Quantification of hyperplasia distal to the lymph node performed in the same manner as in B. D) Number 2/3 mammary glands from 7-week-old WT/PyMT (n = 6) and KO/PyMT (n =

3) mice were stained with anti-phospho histone-H3 (P-H3) antibody to determine proliferation rate. Statistical analysis was done using two-tailed Student's t-test with a p-value threshold of 0.05.

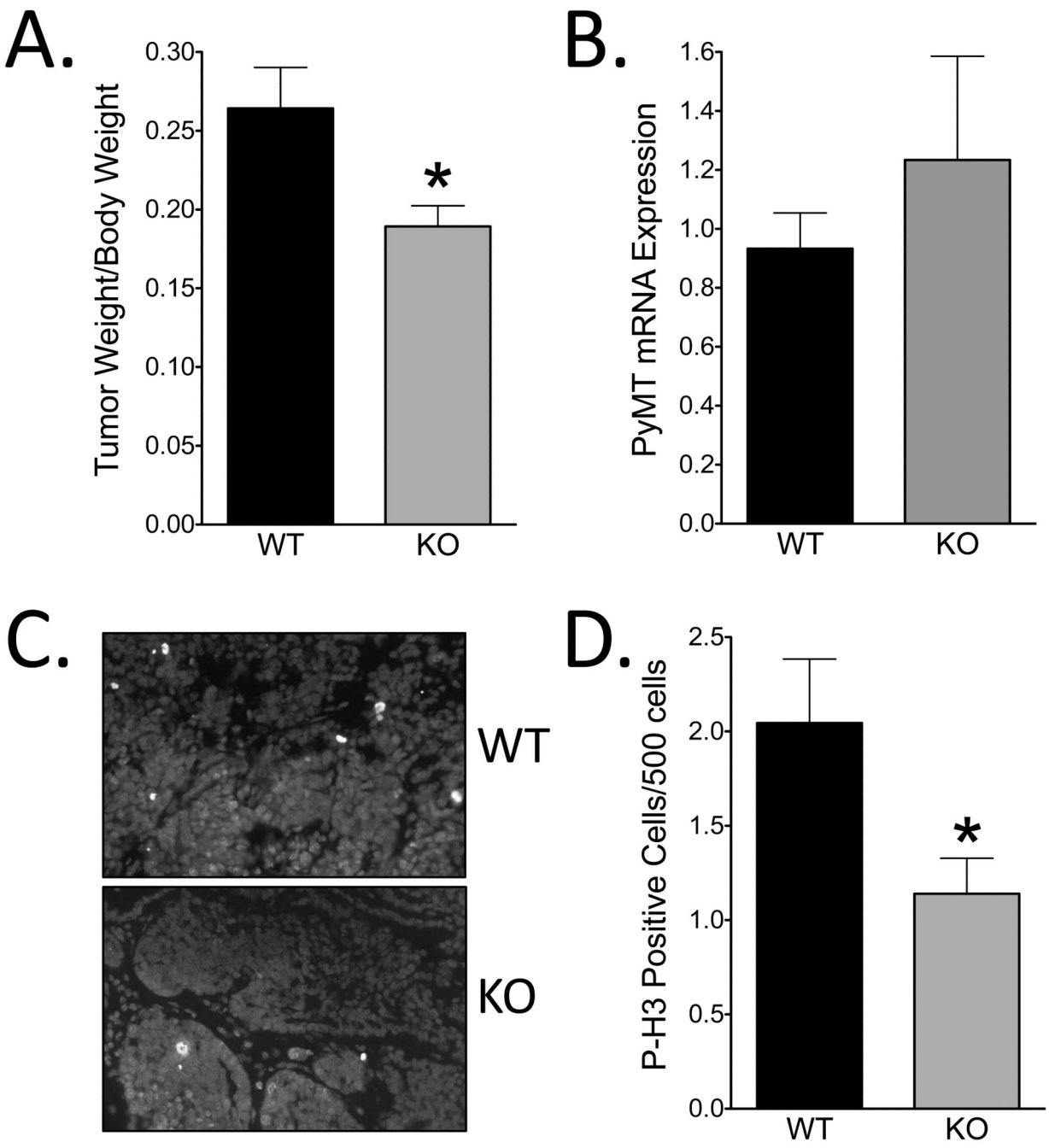

Figure 3. KO/PyMT mice have smaller tumors with decreased proliferation compared to WT/PyMT mice

A) Tumors from WT/PyMT (n = 9) and KO/PyMT (n = 13) mice were resected and weighed at 12-13-weeks-old as a measure of tumor size. B) Quantification of PyMT gene expression relative to cytokeratin 18 from 10-week-old WT/PyMT (n = 4) and KO/PyMT (n = 4) mice. C) Images of P-histone-H3 (P-H3) staining on tumors from 12-13-week-old mice. Blue represents DAPI staining and green represents P-H3-positive cells. D) Quantification of P-H3-positive cells in tumors from WT/PyMT (n = 8) and KO/PyMT (n = 12) mice. Statistical analysis used a two-tailed Student's t-test with a p-value threshold of 0.05.

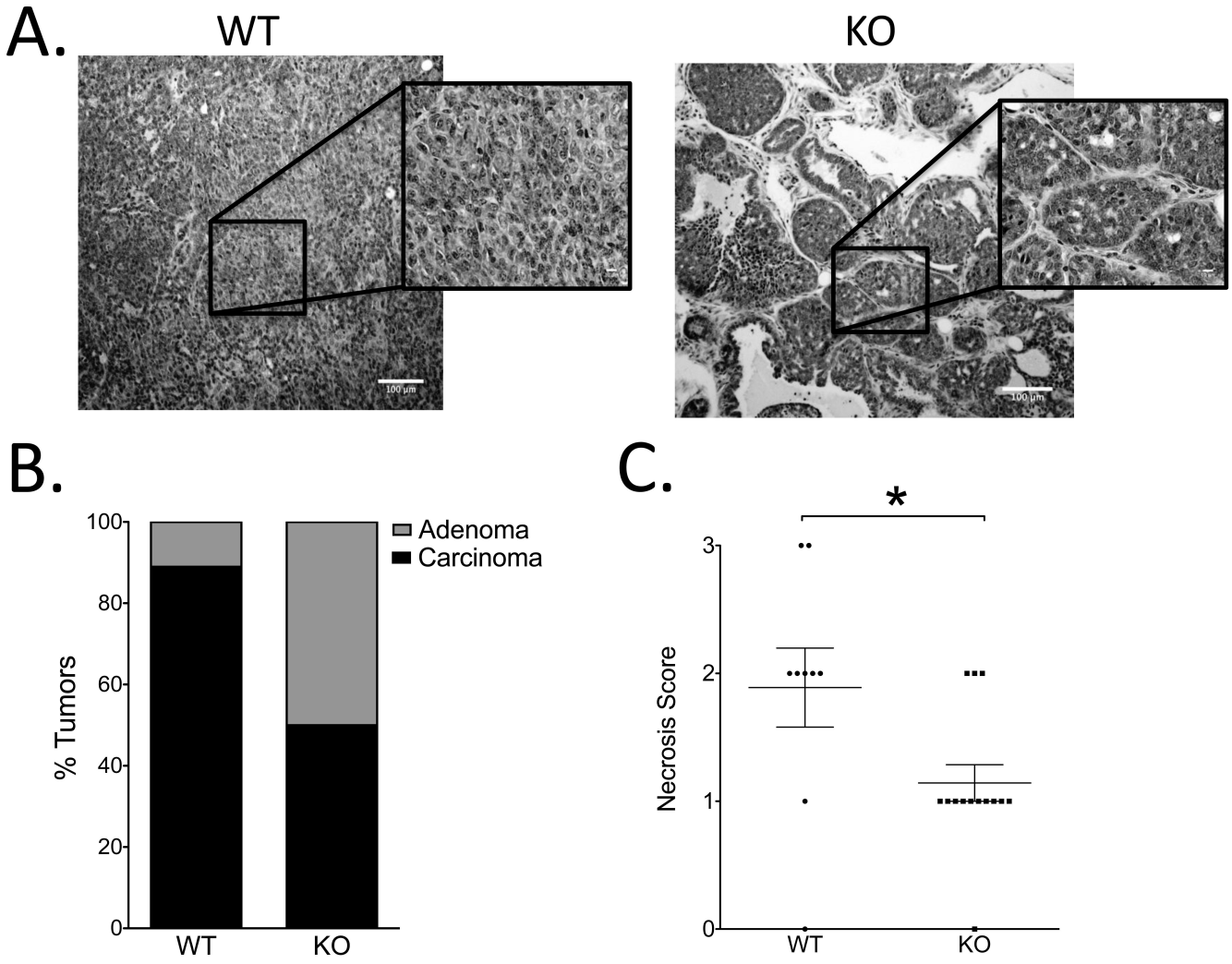

Figure 4. GPER expression is associated with predictors of poor prognosis

A) Representative images of tumors from WT/PyMT and KO/PyMT mice stained with H&E. WT/PyMT mice had little to no acinar definition, whereas acinar structures were present in many tumors from KO/PyMT mice. B) Quantification of tumor grade from WT/PyMT (n = 9) mice and KO/PyMT (n = 14) mice. C) Quantification of the extent of necrosis for WT/PyMT (n = 9) and KO/PyMT (n = 14) mice. Two-tailed Pearson's chi-square test with a p-vale threshold of 0.05 was used for statistical analysis.

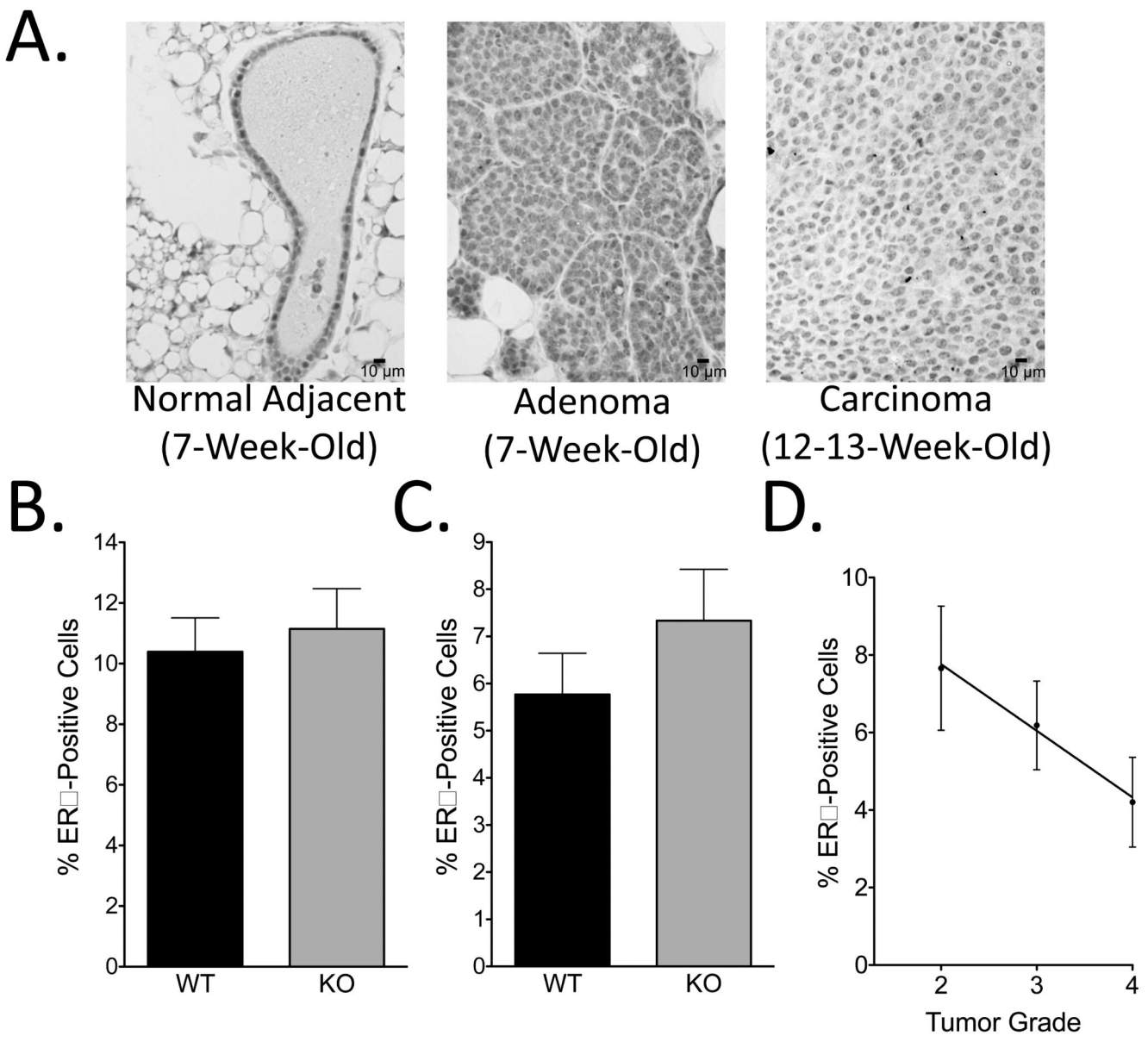

Figure 5. GPER expression does not affect the prevalence of ERα-positive cells

A) Sections (5 μm) of hyperplastic mammary glands from 7-week-old and 12-week-old PyMT mice were immunostained with an anti-ERα antibody. B) Quantitation of ERα$^+$ cells relative to total epithelial cells in 3 random fields in hyperplastic mammary glands from 7-week-old WT/PyMT (n = 5) and KO/PyMT (n = 6) mice. C) Quantitation of ERα$^+$ cells relative to total epithelial cells in 3 random fields in tumors from 12-13-week-old WT/PyMT (n = 8) and KO/PyMT (n = 12) mice. D) Correlation analysis between tumor grade and percent of ERα$^+$ cells from 12-13-week-old WT/PyMT (n = 5) and KO/PyMT (n = 6) mice. Differences in ERα expression were statistically analyzed by two-tailed Student's t-test with a p-value threshold of 0.05. Correlation between ERα expression and tumor grade was analyzed using simple linear regression with a p-value threshold of 0.05.

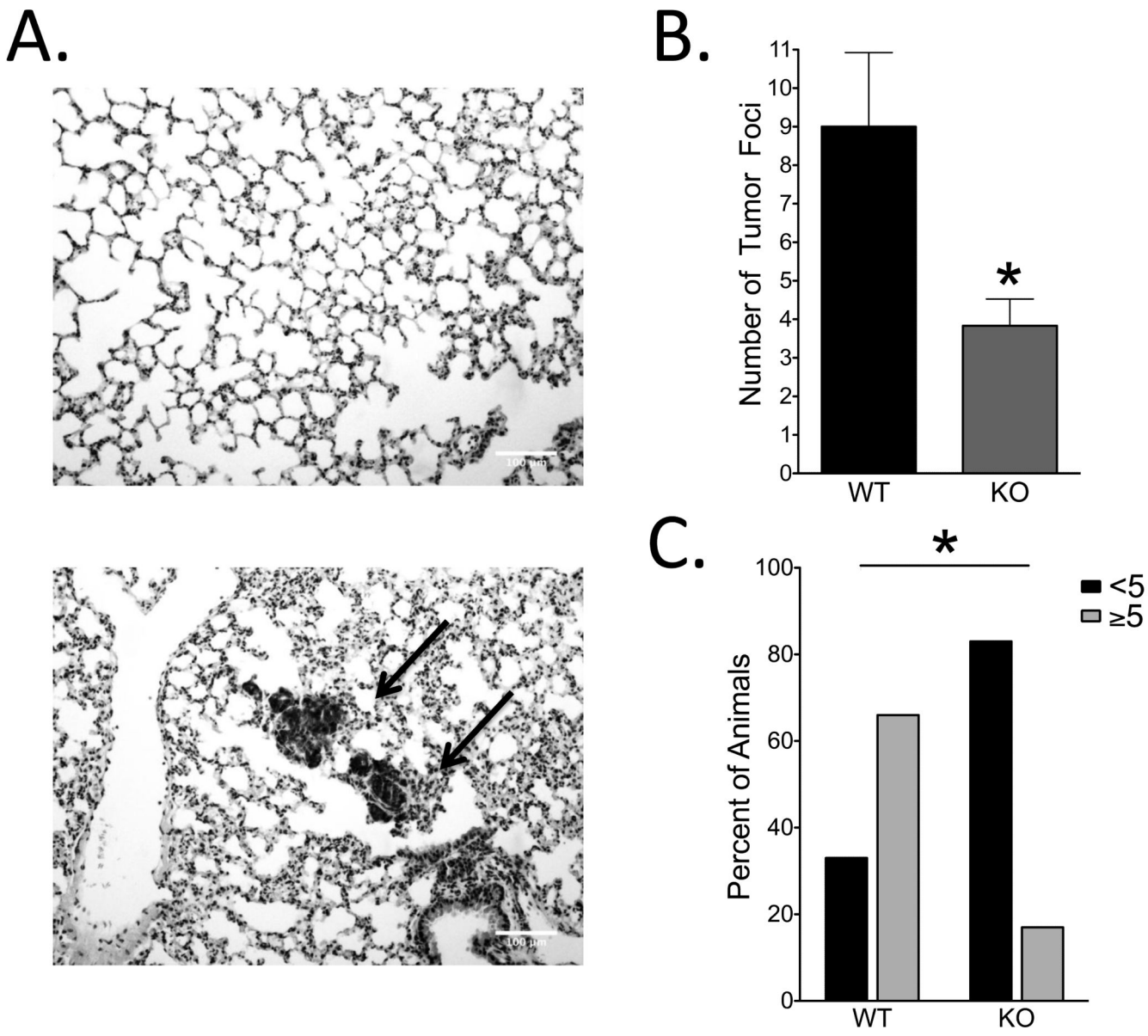

Figure 6. Lack of GPER reduces metastatic burden in PyMT mice

A) Lungs of WT/PyMT and KO/PyMT mice were removed when mice were 12-13-weeks-old and stained with H&E to determine the extent of metastasis. Top image represents normal mouse lung tissue. Bottom image represents mouse lung tissue containing tumor foci (arrows). B) Quantification of the number of tumor foci in WT/PyMT (n = 9) and KO/PyMT (n = 12) mice analyzed by two-tailed Student's t-test with a p-value threshold of 0.05. C) The number of WT/PyMT (n = 9) and KO/PyMT (n = 12) mice exhibiting <5 or ≥5 metastatic foci per lung was analyzed by two-tailed Fisher's exact test with a p-value threshold of 0.05.